A98-31584

ICAS-98-4,3,1

NUMERICAL SIMULATION OF FLUID-STRUCTURE INTERACTION IN AIRCRAFT FUEL TANKS SUBJECTED TO HYDRODYNAMIC RAM PENETRATION

P. Santini, D. Palmieri, M. Marchetti
University of Rome "La Sapienza" - Aerospace Department
Via Eudossiana, 16 - 00184 Rome, Italy

ABSTRACT

The impact of a fragment produced by an uncontained aircraft engine turbine failure against a fuel tank is numerically simulated with the AUTODYN-2D hydrocode. Axial symmetric shapes are considered for the fragment and the tank, because the use of the axial symmetry option makes the 2D simulations equivalent to 3D ones with a strongly reduced computation time. The tank walls loading by the pressure waves generated within the fluid (hydrodynamic ram) is taken into account, in order to understand if the pressure load can rupture the walls causing a large amount of fuel to flow out. Different numerical processors are coupled to simulate the different problem materials: a two dimensional lagrangian processor for the fragment, a thin shell lagrangian processor for the tank walls and an eulerian processor for the fuel. Wall failure is assumed to occur if the material effective plastic strain exceed a limit value.

Introduction

The FAA Aircraft Catastrophic Failure Prevention Research Program

Following a series of tragic civil transport aircraft accidents worldwide since 1979, that resulted in over 1100 fatalities, the Federal Aviation Administration (FAA) established in 1990 (Public Law 101-508) the Aircraft Catastrophic Failure Prevention Research Program. Specifically, the Program stated that improved methodology and advanced technology be applied to assess and prevent catastrophic failures that can result in civil aircraft accidents, the main motivation being that in each accident the devastating consequence may have been prevented.
The goal of the Program is to prevent catastrophic failures and, if prevention is not feasible, to mitigate the effects of such failures to allow for continued controlled flight to a safe landing. Safety of flight depends on each component functioning properly and all functioning together as they were designed to do. Thus, a systems approach is followed in the analysis of each component to address cascading of failures by related components.
The program has three broad categories of aircraft systems: turbine engines, airframes, and flight control systems. In the interests of simplified organization, all aircraft hardware and software are considered to fall into these categories. The vulnerability and survivability of critical aircraft systems that are exposed to threats of single point failures are the major part of this analysis. However, the program's philosophy does not consider the three categories to be independent when viewed from a catastrophic failure prevention perspective. Each category may be influenced by risk assessments in other ones, particularly with regard to the probability of cascading failure modes producing serious secondary damage.

The problem of uncontained engine failures

On rare occasions, aircraft turbine engines fail catastrofically and send into the aircraft fragments that disrupt control, fuel, and propulsion systems and jeopardized the ability of the aircraft to land safely. To enhance the survivability of commercial aircraft in the event of an uncontained turbine engine failure, the FAA is sponsoring a research program in the propulsion field aimed at protecting components of the aircraft that are critical to continued safe flight and landing.
The main research areas of the program are: the characterization of turbine engine failure hazards debris and vulnerability analysis, the evaluation of armor technologies to mitigate uncontained turbine engine failure hazards and the analysis of the effects of fragment penetration in aircraft fuel tanks.

Characterization of debris hazard

A great amount of debris data on existing incidents were gathered at Pratt and Whitney, General Electric and Allied Signal[1]. Data analysis is being conducted in three primary areas: trajectory and debris analysis from the database, penetration analysis using existing penetration equations and debris flyout analysis, in order to identify debris threat characteristics (as debris trajectory, hole size, average hole size, average number of holes per event, etc.) and to estimate the energy levels needed to penetrate typical aircraft structures.

Debris hazard mitigation

An extensive literature summary of 64 reports covering 23 years of research from 1970 to 1993 is presented in ref. 2, to evaluate the existing literature and procedures used to design engine rotors and containment of engine rotors for hazard mitigation. The final sections of the

report provide industry viewpoints and examples of work performed. The general topic of containment of rotating parts in gas turbine engines and protection of the aircraft in the case of noncontainment remains an active area for industry research and development and regulatory interest. The work summarized in this report was to determine some sense of whether a state of the art exists for the problem of designing structural components for containment or shielding functions. To date there is no industry standard for assessing the containment capability of a combined engine and nacelle with proven numerical methods. Additional finite element code development is necessary to match the numerical results with the growing body of experimental data.

When industrial manufacturers were questioned on design methods used when dealing with uncontained rotor burst events, the approach of designing redundant systems and relocating critical components to areas outside of an expected fragment trajectory envelope was mentioned as a primary method. Only in a few cases some design work involving the possible use of structural shielding were related. They mentioned that a possible drawback to the use of shields is that, in certain cases, more serious structural damage results as a consequence of using the shield, because the shield transfers the impact reaction to more structural members. Another mitigation measure indicated was the design of disks to limit the mass of fragments by breaking into small pieces, and the design of directed failure paths.

The Federal Aviation Administration Technical Center-Atlantic City International Airport and the U.S. Army Research Laboratory-Watertown have conducted research and development to identify the state-of-the-art lightweight material concepts that could provide suitable containment and/or isolation from the worst case small turbine engine rotor disc failure hazard[3]. The Naval Air Warfare Center Aircraft Division-Trenton was tasked by FAA Technical Center and ARL to conduct rotor disc burst containment tests on the containment rings designed and fabricated by ARL. Fully bladed Textron-Lycoming T53-L-ll engine power turbine rotor, second stage, was designed and modified to fail into three fragments to evaluate the containment materials.

Concepts, materials and designs that may be useful in developing engine fragment barriers with low added weight and cost are identified in ref. 4. High-strength polymer fibers are confirmed as the advanced material most appropriate for protecting aircraft from engine fragments: furthermore these materials appear to have sufficient flame resistance, water absorption resistance, and thermal and acoustic insulation to serve as building blocks for barriers.

In ref. 5 the development of two fiber reinforced structures for lightweight containment of turbine rotor failures is described. The first is a hybrid core sandwich panel capable of being used both as a part of the airframe or nacelle structure and as a containment panel, if required. The second is a collar or ring placed close to the turbine case wall of a turbofan, turboprop or turboshaft engine. The program focuses on design of these structures to contain a 1 million in-lb. T-53 tri-hub rotor burst using the lowest weight containment structure possible.

These goals are accomplished by sandwich panel and ring design tasks, test article fabrication and spin pit testing. Design modification and subsequent testing develop an understanding of the relationship between reinforcement architecture, static/elastic behavior and dynamic/impact behavior of the ring and panel. Additional spin pit testing is performed to evaluate changes in geometry and panel-to-panel joint designs.

The program results indicate containment structure design characteristics to stop small rotor disk bursts and these results can then guide engine and airframe structure design to minimize the weight/space penalty for containment of internal turbine engine failures.

Hydrodynamic ram description and simulation

One of major risks of uncontained engine failures in commercial aircraft is that they produce high-speed fragments that can impact and damage surrounding structures and equipment. Of particular concern is the possibility of such impacts to fuel tanks.

If a fragment penetrates a wet wall, it slows down as it travels through the fuel due to liquid drag forces. Part of the fragment kinetic energy is converted into fluid mechanical energy, an effect called hydrodynamic ram. The ram pressure loads the tank walls and forces them to bulge and tear, thus increasing the size of the puncture hole produced by the fragment. A large amount of fuel can then flow out of the tank and find its way to an ignition source (such as an hot surface or torn electrical wires), leading to fuel starvation or explosion with an immediate loss of the aircraft.

A typical hydrodynamic ram event is generally considered to consist of a shock phase, a drag phase, a cavitation phase, and an exit phase[6]. The shock phase occurs during initial impact with the fluid at which time the projectile impulsively accelerates the fluid and generates an intense pressure field bounded by a hemispherical shock wave. This shock wave expands radially away from the impact point and may produce petaling of the entrance panel. As the projectile traverses the fluid it transfers a portion of its momentum to the fluid as it is decelerated due to viscous drag. The radial velocity imparted to the fluid during the drag phase lead to the formation of a cavity behind the penetrator: this is often termed the cavitation phase. As the fluid seeks to regain its undisturbed condition , the cavity will oscillate. The time interval during which the exit panel of the fluid cell is perforated by the projectile is referred to as the exit phase.

In previous years a great deal of effort has focused on understanding the causes of hydrodynamic ram; however, the ability to effectively predict the ram effects has been elusive[7]. Computer analyses methods were previously developed to model the ballistic event; however, these methods were finite element-based structure models with simplified fluid pressure loading, and they did not model the fluid structure interaction. Current efforts center on

evaluating the ability to predict hydrodynamic ram using the state-of-the-art hydrocodes.The Hydrodynamic Ram Analytical Methods Program is directed at evaluating the prediction of hydrodynamic ram events, based on state-of-the-art hydrocodes. These hydrocodes utilize Coupled Euler-Lagrange (CEL) techniques such as Arbitrary Lagrange-Euler (ALE) and Smoothed Particle Hydrodynamics (SPH) methodologies. Although these new analysis approaches are computationally intensive, they provide direct modeling of the fluid and structure interaction as the failure of the structure proceeds during the impact event. This program should demonstrate that these codes can be used to accurately predict the hydrodynamic ram event.
The hydrodynamic ram simulation of a steel rod impacting a cylinder filled with water was performed by Kimsey with the EPIC-2 code[8]. All the materials were simulated with lagrangian grids. An erosion criteria was used to allow the formation of voids within the fluid, by permitting total failure of elements that exceeded an equivalent strain of 2.5.

Problem modelization

Geometry

Input data were taken from ref. 9, where the characteristics of various possible fragments of interest from fan, high pressure compressor and turbine are indicated.
The selected simulation case among those reported is the highest kinetic energy fragment from a titanium fan blade. The fragment has a mass of 380 g and a velocity of 258 m/s, so the kinetic energy is 12680 J. The exact fragment geometry is obviously unknown, so it was simulated in three different ways: a long cylinder (LC) with a diameter of 13 mm and a length of 610 mm, a thin cylinder (TC) with a diameter of 155 mm and a length of 4.4 mm, and a sphere (SP) with a diameter of 54 mm.
The target is a fuel cell made of 7075-T6 aluminum alloy 1.5 mm. thick, whose dimensions are 2032x546x432 mm, corresponding to a segment of a Boeing 737 wing between two stiffeners. The cell is supposed to be completely filled with fuel.
Fragment is considered to normally impact the tank along the directions of its two major dimensions, that is 2032 mm (case a) and 576 mm (case b). Cases in which tank length along impact direction is 2032 mm are indicated with LC-a, TC-a and SP-a for long cylinder, thin cylinder and sphere respectively, while cases in which tank length along impact direction is 546 mm are indicated with LC-b, TC-b and SP-b. Cylinders always impact the tank with the impact velocity vector directed along their axis. The initial configurations of selected cases are represented in figure 1.
Analysis was performed with the AUTODYN-2D hydrocode using of the axial symmetry option, that makes the 2D simulations equivalent to 3D ones on axisymmetric projectiles and targets, but with a strongly reduced computation time. Then the axisymmetric shapes of the fragment were correctly simulated, while the fuel cell was simulated as a cylinder, having a diameter of 546 mm and a length of 2032 mm in case a, and a diameter of 2032 mm and a length of 546 mm in case b.
The hydrodynamic ram analysis was performed in ref. 9 using a constant drag coefficient between the fragment and the fluid, assuming the disturbances in the fluid to obey the linear acoustic wave equation. A fracture mechanic based failure criterion was used to predict wall failure. Impact was considered to occur from the bottom to the top wall. The results obtained indicate failure of the wall for the thin cylinder and the sphere but not for the long cylinder.

Numerical processors coupling

Unlike in ref. 8, where only lagrangian grids were used, in the present work the different materials involved in the problem were simulated with different numerical processors, utilizing the AUTODYN capability to model different domains of a physical problem with different numerical techniques most appropriate for that domain. These different domains are then coupled together in space and time to provide an optimized solution.
The fragment was modeled with a two dimensional lagrangian grid. Tank walls were simulated with a thin shell lagrangian model, because a prohibitively small timestep would be required for a two dimensional continuum approach of thin shell structures. Although thickness is considered in the shell formulation, it is not included in the geometric representation of the shell and does not enter into the timestep calculation. The two lagrangian grids interact across an impact/slide interface. The fluid fuel, that is subjected to very large flow and deformation, was modeled with an eulerian grid. The lagrangian grids interact with the eulerian grid across an Euler-Lagrange interface, in which the Lagrange grid acts a geometric constraint to the Euler grid while the Euler grid provides a pressure boundary to the Lagrange grid.

Material models

Materials behaviour is basically simulated in the hydrocode theory with an equation of state (EOS), that expresses the value of hydrostatic pressure as a function of density and internal energy, and a constitutive relation between the deviatoric stresses and strains.

The shock EOS was used to model the titanium fragment and the fuel. This EOS is derived from many dynamic experiments making measurements of material particle velocity u_p and shock velocity U. It has been found that for most solids and many liquids over a wide range of pressure there is an empirical linear relationship between these two variables:

$$U = c_0 + su_p$$

where c_0 is the sound speed and s is the slope parameter. The shock EOS is then expressed in a Mie-Gruneisen form based on the previous relation:

$$p = \frac{\rho_0 c_0^2 \mu(1+\mu)}{[1-(s-1)\mu]^2} + \Gamma\rho\left\{e - \frac{1}{2}\left[\frac{\mu c_0}{1-(s-1)\mu}\right]^2\right\}$$

where $\mu=\rho/\rho_0 - 1$ and Γ is the Gruneisen parameter. The following values were used in the simulation (as no specific data about s and Γ were found for jet fuel, the values relative to water were used for these parameters).

Material	ρ (g/cm^3)	c_0 (m/s)	s	Γ
TITANIUM	4.42	5020	1.536	1.23
FUEL	0.82	1320	1.75	0.28

TABLE 1: EOS parameters

An elastic-perfectly plastic (constant yield stress) constitutive model was chosen to take into account for the shear strength of blade and tank solid materials. A failure criterion was then used, assuming that failure in a cell occurs when the plastic strain exceeds a specified limit value: when this happens, the stress deviators are set to zero and in post-failure flow in that cell the material cannot sustain any shear strength or any negative hydrodynamic pressure. Obviously no shear strength and failure were considered in the fuel model. Parameter values used for the shear modulus G, the yield stress Y and the failure strain ε_R are reported in table 2.

Material	G (Gpa)	Y (Mpa)	ε_R
TITANIUM	43.4	850	0.08
Al 7075-T6	26.7	420	0.11

TABLE 2: constitutive and failure model parameters

Fragment penetration into fuel tank is allowed by removing from the calculation shell elements that have reached the specified failure strain value.

Results

The features of the impact strongly depend on the fragment shape. When the tank is impacted along its shortest dimension (cases LC-b, TC-b and SP-b) the front wall is always perforated, that is the fragment enters inside the tank. When the impact occurs along the greatest tank dimension the front wall has a smaller surface, and it is perforated only by the sphere and the long cylinder (cases LC-a and SP-a), while the thin cylinder (case TC-a) ricochets against the wall without perforating it.

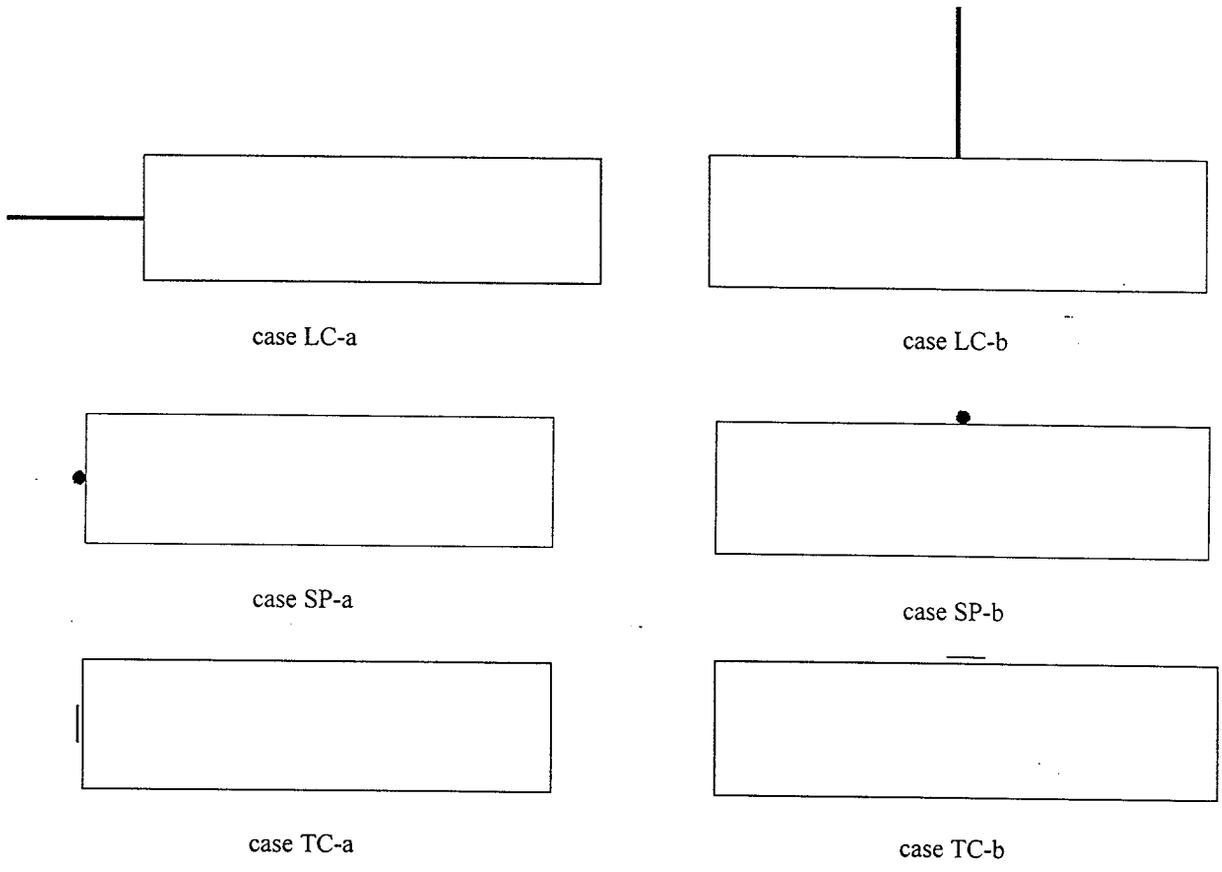

FIGURE 1: simulation cases

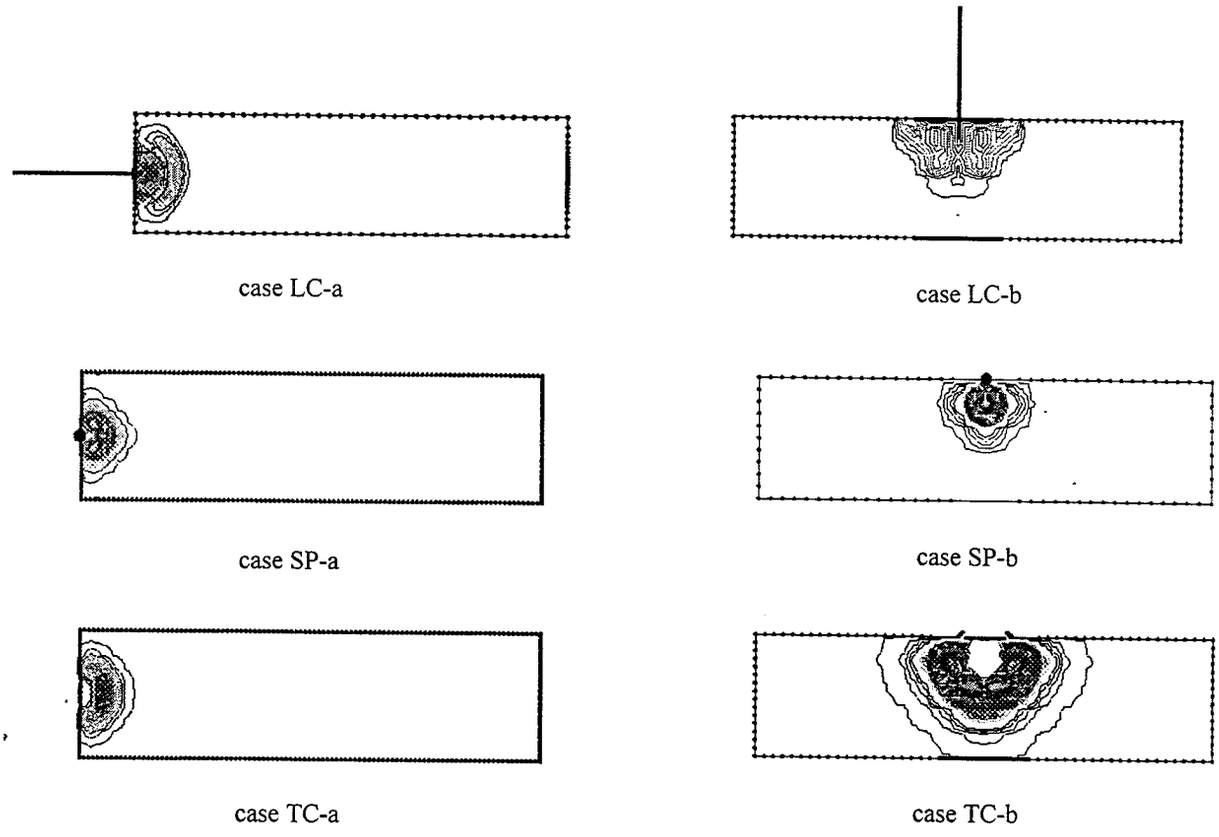

FIGURE 2: pressure waves patterns

When the fragment penetrates inside the tank, it does not exit perforating the back wall in all cases: this always happens for the long cylinder (cases LC-a and LC-b) and only for the sphere when it impacts the tank along the shortest dimension (case SP-b). When the tank is impacted by the sphere along the major dimension (case SP-a) or by the thin cylinder along the smaller one (case TC-b), the drag forces developing during the fragment penetration within the fluid completely decelerate the impactor before it reaches the back wall.
In cases where the fragment cannot reach the back wall and exit the tank the highest quantity of energy is transferred to the fluid. Also in case TC-a, where the fragment does not penetrate the front wall, it transfers through the wall a great amount of its energy to the fluid. In all these cases the residual velocity of the fragment is practically reduced to zero.
The long cylinder is the shape that, having the smaller cross section with respect to the impact direction, transfers to the fluid the smaller quantity of energy: this quantity is higher in the case of penetration along the major tank dimension, because the fragment stays in contact with the fluid for a larger time. The residual velocities are the highest for these two cases.

The sphere impacting the tank along the smaller dimension (case SP-b) perforates the back wall and exit with a quite high residual velocity, but it also transfers to the fuel a considerable part of its initial energy. Table 3 shows for each case the quantity E_F of the initial fragment energy E_I transferred to the fluid and the residual velocity of the fragment V_R with respect to the initial velocity V_I.

Case	E_F/E_I	V_R/V_I
LC-a	0.26	0.78
SP-a	0.70	0.07
TC-a	0.67	-
LC-b	0.01	0.98
SP-b	0.45	0.62
TC-b	0.59	0.03

TABLE 3: fuel energy and fragment residual velocity

When the front wall is impacted by the fragment it compresses the inner fluid, generating pressure waves that propagate with an approximately hemispherical pattern. The expanding waves reach the inner surfaces of the walls, making them bulge under the pressure load. In figure 2 the wave patterns are reported before they reach the walls.

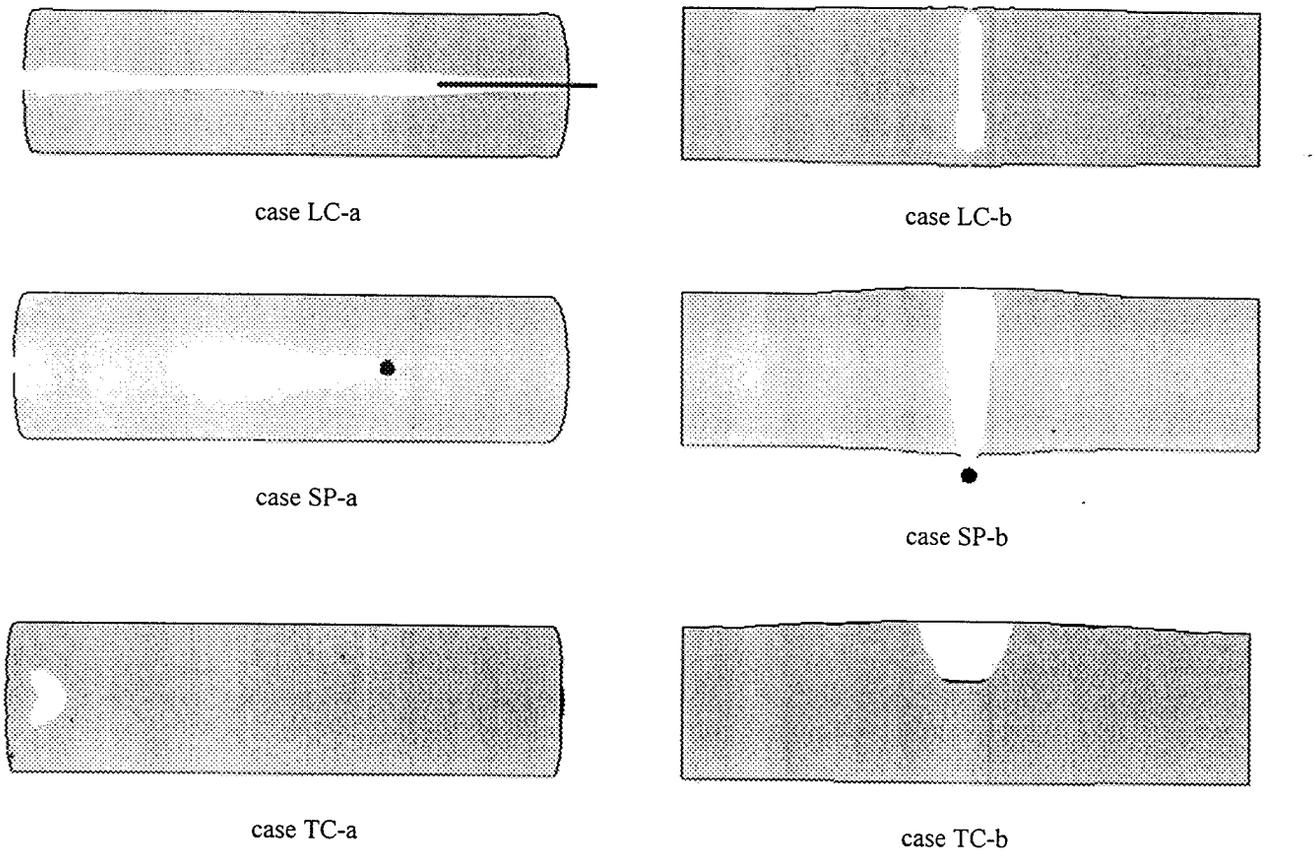

FIGURE 3: cavity formation within the fluid

The formation of the cavity following the penetrating fragment is well simulated (see figure 3). When the fragment velocity reduction is small, the penetration time is short enough that the cavity last also after the fragment has completely passed through the tank length (cases LC-a, LC-b and SP-b). If the fragment enters the tank but it is stopped before reaching the back wall, after a certain time the cavity begin to close "following" the penetrator after its passage (cases SP-a and TC-b). It is interesting to observe that also when the fragment does not penetrate the tank at all (case TC-a), the pressure waves generated during the impact against the wall lead to the formation of a cavity, that expands away from the impact point and then tends to close.

When the pressure waves generated within the fluid at the impact point reach the tank walls load them and make them bulge, causing petaling of the entry panel. The final shape of deformed tank is shown in fig. 4: the higher deformations are always located on the front and back walls in the zone of impact axis.

The front and back wall hole diameters together with the fragment diameter are reported in table 4. The ratio between the final hole and the fragment diameter is in the range from 1.2 to 1.5. The determination of the final hole diameter is very important because it influences the quantity of fuel that can flow out from the tank.

Case	Fragment diam. (mm)	Front hole diam. (mm)	Back hole diam. (mm)
LC-a	13	20	17
SP-a	54	66	-
TC-a	155	-	-
LC-b	13	21	20
SP-b	54	61	57
TC-b	155	200	-

TABLE 4: hole diameters

In table 5 the maximum bulge (that is the maximum displacement along the impact direction) and the maximum plastic strain on the front and back wall are reported.

It has to be noted that the highest values of the plastic strain have been observed on the edge of wall holes, obviously when a hole is present. Thus an increase of wall failure seems to be possible due to an higher energy impact, that could generate a more intense pressure field under which the hole size could enlarge. The wall would

result then weakened, and could be subjected to further deformation under the applied pressure load.

Case	Max. front wall bulge (mm)	Max. front wall strain	Max. back wall bulge (mm)	Max. back wall strain
LC-a	33	0.08	40	0.09
SP-a	25	0.03	55	0.03
TC-a	31	0.03	32	0.05
LC-b	10	0.08	14	0.07
SP-b	50	0.07	52	0.09
TC-b	66	0.09	39	0.01

TABLE 5: maximum wall bulge and strain

Also the walls that have not been penetrated in the considered cases could be subjected to higher deformation because of a more intense impact load, but it seems probable that failure happens in the weaker zone of the structure (i.e. near the holes), considering also that plastic strain values on undamaged walls are lower than those near hole edges. If the pressure load was high enough penetration could occur on walls that have resulted undamaged in the case of present work, thus increasing the probability of a failure.

Conclusions

The hydrodynamic ram loading on the walls of an aircraft tank impacted by an uncontained engine debris was numerically simulated with the use of a 2D hydrocode.
Different numerical processors were coupled to simulate the different materials involved in the problem with the most appropriate technique.
Through the time integration of conservation equations it is possible to determine the values of physical variables in each point at every time, such as material velocity, fluid pressure and wall stresses and strains, this allowing a continuous monitoring of structure damage.
The results indicate that more intense pressure waves, generated by an higher energy impact, could enlarge the size of the hole produced by fragment penetration, thus weakening the structure and increasing the probability of a failure growth under the applied load.

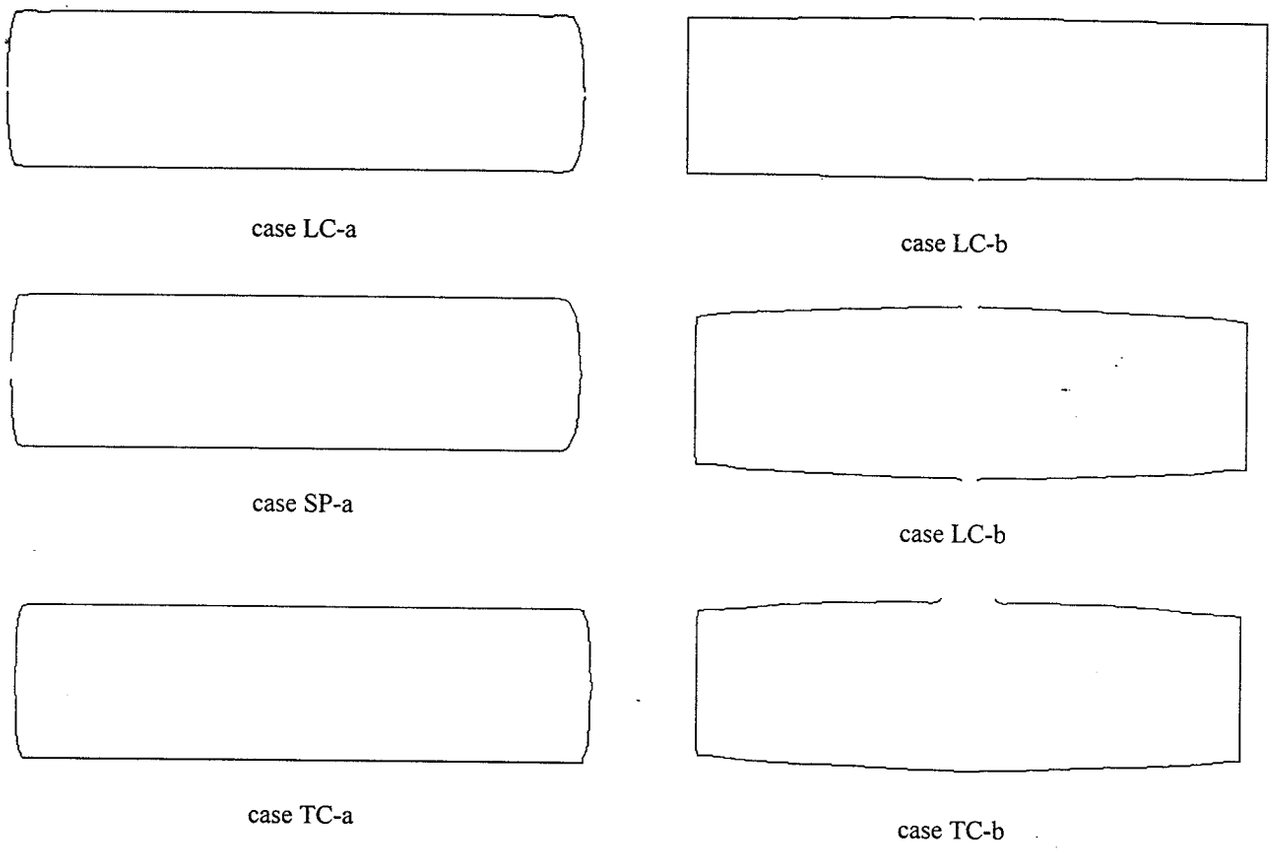

FIGURE 4: final tank shape

REFERENCES

1 "Characterization of Turbine Engine Failure Hazards Debris & Vulnerability Analysis", Federal Aviation Administration Interagency Agreement No. DTFA03-95-X-90019.

2 "Design Procedures and Analysis of Turbine Rotor Fragment Hazard Containment", Report DOT/FAA/AR-96/121.

3 "Evaluation of Lightweight Material Concepts for Aircraft Turbine Engine Rotor Failure Protection", Report DOT/FAA/AR-96/110.

4 "Advanced Armor Technology: Application Potential for Engine Fragment Barriers for Commercial Aircraft", Report DOT/FAA/AR-97/53.

5 "Fiber Reinforced Structures for Turbine Engine Fragment Containment (Phase II)", Report DOT/FAA/AR-95/110.

6 J.A. Zukas et al., "Impact Dynamics", John Wiley & Sons Inc. Ed., 1982, pp.397-398.

7 Joint Aeronautical Commanders' Group, Joint Technical Coordinating Group On Aircraft Survivability, Aircraft Survivability Newsletter Winter 1995/96, "Year In Review".

8 K.D. Kimsey, in Proceedings of "1980 Summer Computer Simulation Conference", Seattle, WA., Aug. 25-27, 1980, Simulation Councils Inc., La Jolla, California.

9 "The Potential for Fuel Tank Fire and Hydrodynamic Ram Initiated by Uncontained Engine Debris on Commercial Aircraft", Report DOT/FAA/AR-96/95.